MODIFICATION OF ZSM5 TYPE ZEOLITES WITH H_3PO_4

Johannes A. Lercher, Gerd Rumplmayr and H. Noller
Institut für Physikalische Chemie, Technische Universität Wien,
Getreidemarkt 9, A-1060 Vienna, AUSTRIA

ABSTRACT

The effects of H_3PO_4 upon the acidic and catalytic properties of ZSM5 zeolites were investigated. Pyridine and ammonia were found to adsorb on the same sites indicating no sterical constraints for the former. Two desorption states were observed, denoted as α and γ. Comparison of t.p.d. and i.r. spectra suggests that the first desorption rate maximum is due to pyridine (ammonia) desorbing from very weakly acidic sites, the second (γ) is due to molecules desorbing from Bronsted acid sites. The strength of the latter sites decreased with increasing H_3PO_4 loading. Strong Bronsted acid sites have been found to be indispensable for hydrocarbon formation from methanol. Zeolites with 5 and 8 w % H_3PO_4 did not catalyze hydrocarbon formation at a considerable rate. Because the energy of activation for n-hexane cracking increased strongly with H_3PO_4 loading, we concluded that the sites decreased in strength and we could exclude diffusional constraints as cause for reduced activity with increasing P-content.

INTRODUCTION

According to Sanderson's concept of electronegativity (1), oxides of higher intermediate electronegativity should exhibit sites of higher acid strength. Therefore one expects to find also with zeolites higher acid strength with increasing silicon-to-aluminum ratio. Indeed , Kazanskii et al. (2), calculating relative values for the deprotonation energies of bridging hydroxyls in models beeing representative for samples of Si/Al ratios from 1 to 4, found deprotonation energy to decrease with increasing Si/Al ratio, which accords with the results of Jacobs and Mortier (3). These theoretical calculations and the experiments reported by Jacobs et al. (4) are discussed by Mortier et al. (5). Lercher and Noller (6) have shown for silica-alumina-magnesia mixed oxides that, after acetone was adsorbed, the wavenumber of (non Bronsted) terminal hydroxyl groups was displaced the more the higher the intermediate electronegativity of the investigated mixed oxide was. This increase indicates increasing acid strength, i.e. increasing electron pair acceptor (EPA) strength , in the same order (7).

Therefore one would expect that surface treatment of a zeolite with compounds of high electronegativity like H_3PO_4 would increase the acid strength. In contrast, the catalytic experiments reported with phosphorous modified zeolites suggested a decrease in acid strength rather than the reverse (8,9). Derouane et al. also reported (10) that incorporation of boron into tetrahedral sites (substituting Al^{3+}) decreased the acid strength of the resulting zeolite.

In order to study these effects in some greater detail we have prepared a series of ZSM5 zeolite catalysts loaded with increasing amounts of H_3PO_4. The acidic properties of these materials were studied by means of pyridine adsorption and desorption (i.r transmission-absorption spectroscopy and temperature programmed desorption) as well as by reactions with methanol and n-hexane and are compared with those of pure ZSM5 and pure $AlPO_4$-5 molecular sieve (11).

EXPERIMENTAL

Catalysts and reagents. ZSM5 zeolite (Silicalite, 98.76 w% Si, 1.13 w% Al, 0.11 w% Na) was obtained from Union Carbide, Linde Division, New York (LOT # 8496-68). To impregnate the zeolites, 10 g were suspended in 100 ml distilled water and the desired amount of H_3PO_4 was added. This suspension was refluxed for 2 hours and then the water was evaporated under reduced pressure. The remainder was dried at 373 K and tempered at 773 K for 1 hour in air. The resulting catalysts contained 1, 2, 5 and 8 % H_3PO_4 by weight, denoted as ZSM5P1, ZSM5P2, ZSM5P5 and ZSM5P8, respectively in the following. $AlPO_4$-5 (AlPO) was prepared according to (11). The BET surface areas were 365, 304, 287, 295, 230 and 290 $m^2.g^{-1}$ for ZSM5, ZSM5P1, ZSM5P2, ZSM5P5, ZSM5P8 and AlPO, respectively. The crystallinity of all materials was checked by X-ray diffraction analysis and no other lines than those characteristic of ZSM5 or AlPO were observed.

Pyridine, methanol and n-hexane have been obtained from Merck (uvasol grade). All gases used, had at least 99.995 vol% purity.

Infrared measurements. The oxides were investigated by means of the transmission - absorption technique. The i.r. cell was constructed to permit all sample handlings to be done under vacuum and was described previously. For investigation, the zeolites were pressed into thin self supporting wafers ($p=10^8$-3.10^8 Nm^{-2}). The spectra were recorded from 4000 - 1000 cm^{-1} using a Perkin Elmer 325 type i.r. spectrophotometer with 3 cm^{-1} resolution at 3600 cm^{-1}.

Temperature programmed desorption (t.p.d.) measurements. T.p.d. was carried out in vacuum (below 10^{-1} Pa) using a temperature increment of 10 $K.min^{-1}$ in the range between 300 K and 1000 K. The reactor was a quartz glass tube connected with a vacuum pump and a Balzers 311 quadrupole mass spectrometer for detection of the desorbed species. The mass spectrometer was controlled by a Digital MINC computer. For further details see reference (12). The sample (50

mg) was calcined in the t.p.d. reactor at 873 K for one hour, cooled to ambient temperature and contacted with the adsorbent (1.8 kPa pyridine, 2.5 kPa ammonia). Then the sample was evacuated at ambient temperature for 30 to 60 minutes and the t.p.d. started subsequently.

Catalytic measurements. Measurements were carried out in continuous flow mode with methanol at a feed rate of $5.6.10^{-3}$ mol.h^{-1} and a partial pressure of 15.4 kPa and with n-hexane at a feed rate of 7.10^{-3} mol.h^{-1} and a partial pressure of 15.9 kPa. The total pressure was 1 bar and 0.1 g catalyst were used. The products were kept at 400 K and injected into the G.C. column (Chromosorb 102) via a six-port-valve. A Hewlett Packard 5840A gaschromatograph with FID was used. For n-hexane cracking the differential method of data analysis was employed.

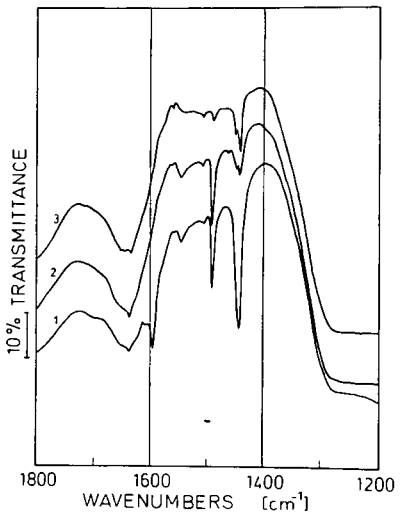

Fig.1. Pyridine on ZSM5
(1) 0.001 Pa, 298K, 1h, (2) 0.001 Pa, 573K, 1h, (3) 0.001 Pa, 773K, 1h

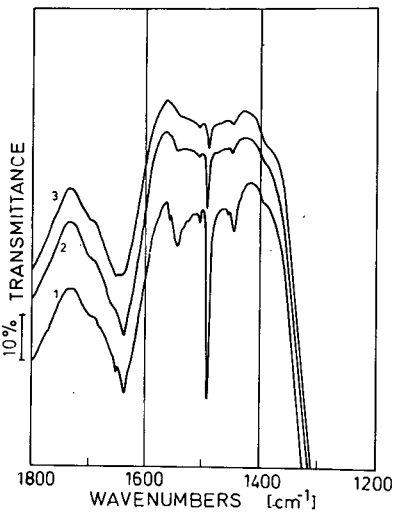

Fig.2. Pyridine on ZSM5P5
(1) 0.001 Pa, 573K, 1h, (2) 0.001 Pa, 573K, 1h, (3) 0.001 Pa, 773K, 1h

RESULTS

I.r. adsorbate spectra of pyridine. The wavenumbers of the 8 a,b and 19 a,b vibrations of pyridine adsorbed on the zeolites are compiled in table 1. Adsorbate spectra with pure ZSM5 and ZSM5P5 can be seen in figure 1 and 2. After admission of 1860 Pa pyridine into the i.r. cell at ambient temperature all adsorbate spectra exhibited intense 19 b bands around 1438 cm^{-1} indicating weak interaction between the surface and the pyridine molecules. Furthermore, it is interesting to note that the relative intensity of the 1540 cm^{-1} band (due to protonized pyridine molecules) is rather low under these conditions. When the i.r. cell was evacuated (10^{-2} Pa) it increased in intensity, while the 19 b band (1438 cm^{-1}) decreased strongly. This could be observed with all zeolites investigated. Two 19 b bands (1450 and 1445 cm^{-1}) were found with pure ZSM5 but

only one (near 1448 cm^{-1}) with H_3PO_4 treated molecular sieves. The relative intensity of this band decreased with increasing H_3PO_4 loading. $AlPO_4$-5 exhibited, however, a rather strong band at this wavenumber. The band at 1540 cm^{-1} (not observed with $AlPO_4$-5) had a markedly lower stability with ZSM5P5 and ZSM5P8 than with the other zeolites (see figure 1 and 2). The wavenumber itself showed no significant variation.

TABLE 1

Wavenumbers (cm^{-1})of 8a,b and 19a,b bands of pyridine adsorbed on ZSM5 samples

	298K, 1.6kPa	298K, ev.	473K, ev.	673K, ev.
ZSM5	1640,1595,1585	1640,1595	1640,1595	1640,1545
	1545,1490,1482	1545,1490	1545,1490	1490,1450
	1443,1438	1443	1450,1443	1445
ZSM5P1	1640,1602,1598	1640,1595	1640	1640
	1585, 1545	1545	1545	1545
	1490,1485,1438	1490,1448	1490,1448	1490,1448
ZSM5P2	1640,1602,1598	1640,1600	1640	1640
	1588,1582,1545	1545,	1545	1545
	1490,1485,1438	1490,1448	1492,1448	1492,1448
ZSM5P5	1640,1602,1598	1640	1640	1640
	1585,1545	1545	1545,1490	1490
	1490,1482,1438	1490,1448	1448	1448
ZSM5P8	1640,1602,1598	1640	1640	1640
	1585,1545	1545,1490	1545,1490	1490
	1490,1482,1438	1448		
AlPO	1609,1577	1610,1577	1620	1620
	1492,1480	1491	1490	1490
	1447,1438	1448	1449	1449

T.p.d. of pyridine. Pyridine desorbed in two steps causing one desorption rate maximum at 373 K and another between 758 K and 778 K. These adsorption states are denoted as α and γ peak in the following in accordance with (13,14). The maxima are compiled in table 2, the plots can be seen in figure 3. While the α peak showed no effect of H_3PO_4 treatment, the γ peak shifted gradually to lower temperatures with increasing H_3PO_4 loading. The lower maximum of the rate of desorption indicates a decrease of the energy of activation of desorption.

T.p.d. of ammonia. The temperatures of the maxima of desorption rate are collected in table 2, the temperature dependence of the desorption rate is

plotted in figure 4. The types of adsorption states are identical with those found for pyridine, the maxima, however, were found at somewhat lower temperatures and the intensity of the α peak was significantly lower than with pyridine. With increasing H_3PO_4 loading the maximum of the γ peak was found at lower temperatures, present only as a weak shoulder with ZSM5P5 and ZSM5P8. No γ peak was detected with $AlPO_4$-5.

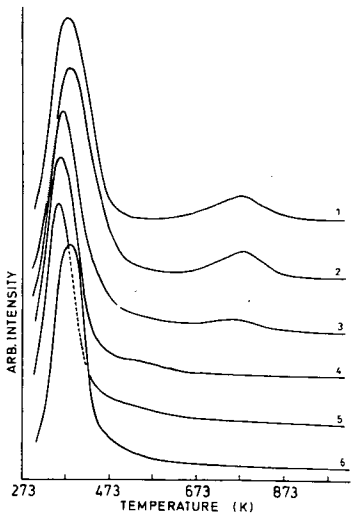

Fig.3. T.p.d. of pyridine

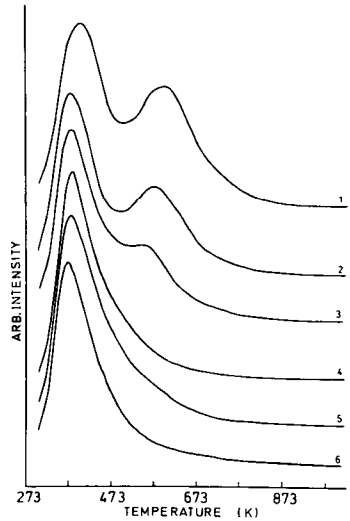

Fig.4. T.p.d. of ammonia

(1) ZSM5, (2) ZSM5P1, (3) ZSM5P2, (4) ZSM5P5, (5) ZSM5P8, (6) AlPO

TABLE 2

Maxima of desorption rates of pyridine and NH_3 (K)

	ZSM5	ZSM5P1	ZSM5P2	ZSM5P5	ZSM5P8	AlPO
Pyridine	383,778	381,778	370,758	367	360	373
Ammonia	383,598	379,580	378,547	383	383	378

Reactions with methanol. Figures 5-7 summarize the main product selectivities and activities of reactions of methanol over ZSM5, ZSM5P1 and ZSM5P5. Under the reaction conditions (15.4 kPa methanol) used, a high preference to olefins is expected and was observed. The conversion to hydrocarbons reached 89.5, 93.6, 4.6 and 0.4 mol % over ZSM5, ZSM5 1, ZSM5P5 and $AlPO_4$-5, respectively. For the latter two zeolites even at temperatures higher than 673 K no significant amounts of hydrocarbons were found, i.e. methanol was completely converted into dimethylether.

In order to establish the nature of active sites the catalyst was partial-

ly poisoned with pyridine. For one set of experiments, pyridine was adsorbed and the temperature was ramped to 673 K with an increment of 10 K per minute. This catalyst converted methanol only to dimethylether. If, however, the temperature was ramped to 873 K the original activity and selectivity of the zeolite was restored.

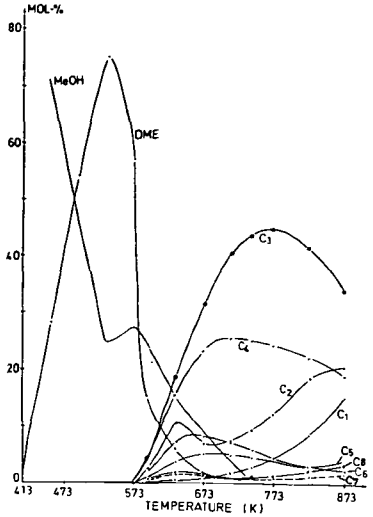

Fig.5. Methanol over ZSM5

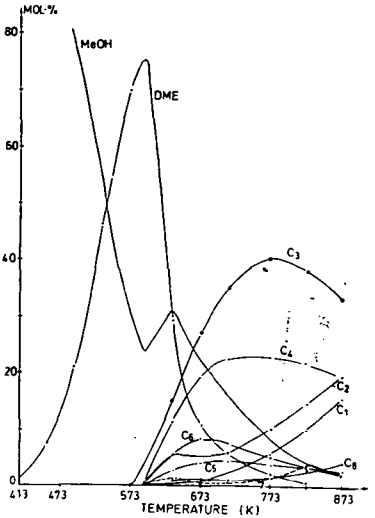

Fig.6. Methanol over ZSM5P1

Cracking of n-hexane. For further characterization of the acidic properties, cracking of n-hexane was performed in a differentially operated continuous flow reactor. The turnover frequencies (TOF) at 673 K (number of molecules n-hexane cracked per second and unit area of the zeolite), the apparent energy of activation and the product distribution are compiled in table 5. The TOF decreases from $1.1 \cdot 10^{15}$ over ZSM5 to $1.9 \cdot 10^{13}$ over ZSM5P5. Furthermore the molar ratio of ethane and ethene reverses from ZSM5P2 to ZSM5P5 indicating a change in mechanism.

TABLE 3

Cracking of n-hexane at 673 K

	TOF	E_a (kJ/mol)	Product distribution				
			C1	C2	C3	C4	C5
ZSM5	$1.1.10^{15}$	78.9	0.79	21.75	48.46	24.25	4.75
ZSM5P1	$8.3.10^{14}$	110.4	0.75	23.36	42.68	27.99	5.22
ZSM5P2	$4.5.10^{14}$	120.1	0.74	27.00	51.16	13.40	7.70
ZSM5P5	$1.9.10^{13}$	170.9	1.54	26.15	33.85	10.77	27.69

DISCUSSION

Adsorption of pyridine reveals two kinds of acid sites with H_3PO_4 modified zeolites, Lewis acid sites and Bronsted acid sites. It was outlined in the introduction that using Sanderson's electronegativity model one expects to find an increase in acid strength upon modification with highly electronegative compounds. The results, however, suggest that the reverse happens.

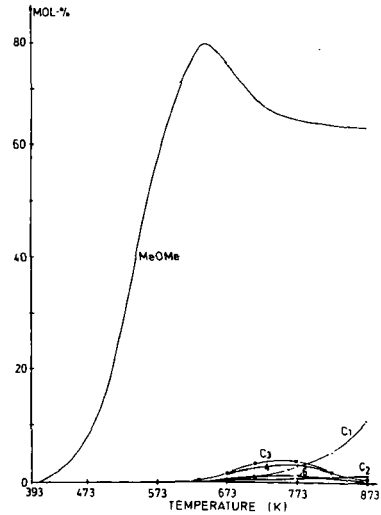

Fig.7. Methanol over ZSM5P5

The strength (the apparent acceptor strength (15)) of the Lewis acid sites was somewhat diminished after the first amounts of H_3PO_4 were deposited on the zeolite. Only one wavenumber of the 19 b vibration (1448 cm^{-1}) was found, instead of two with pure ZSM5 (1450, 1445 cm^{-1}). This indicates a slight decrease of the EPA strength (16) and it may be explained by the better shielding of the phosphorous atom with oxygen compared to Al^{3+}. Once this is achieved (by impregnation with 1 w % H_3PO_4) the wavenumber did not change any further, indicating a similar EPA strength independent of loading. The number of these sites, judged from the relative intensity of the band at 1448 cm^{-1}, decreased with loading.

The relative intensities of the band near 1540 cm^{-1} (due to protonized pyridine molecules) slightly increased with P-content. Hence the density of Bronsted acid sites seems to increase H_3PO_4 is deposited. The thermal stability of the pyridinium ions decreased, however, with increasing loading. This suggests decreasing acid strength.

If these i.r. adsorbate spectra are compared with the rate of desorption during t.p.d., it is possible to correlate the i.r. adsorbate structures with the adsorption states (for details see (14)). The α state is caused by pyridine desorbing from very weakly acidic sites. Adsorption sites for these molecules

certainly include OH groups. For pure ZSM5, a comparison of the i.r. spectra after evacuation at 673 K and 873 K (the temperature intervall of the γ t.p.d. peak) reveals that the intensity of the pyridinium band (1540 cm^{-1}) changes significantly, suggesting that these pyridine molecules desorb from Bronsted acid sites. The absence of a desorption peak around 773 K with zeolites having higher H_3PO_4 loading accords nicely with the lower thermal stability of the pyridinium ion as found by i.r. adsorbate spectra.

Because Topsoe et al. (13) had reported similar adsorption states using ammonia as a probe molecule, but rejected pyridine as not suitable, we also performed ammonia desorption experiments. We found that the estimated amount of NH_3 desorbing from the α state is smaller than that of pyridine and that all desorption rate maxima are shifted to lower temperatures with respect to pyridine. This indicates an overall weaker interaction of ammonia. It also suggests that pyridine is able to adsorb on all sites within the catalyst pore system.

In order to check this, we performed partial poisoning experiments (for details see (14)) by reactivating ZSM5 zeolite (after pyridine adsorption) at 673 K and 873 K, respectively. Over both catalysts methanol was converted. The temperatures were chosen so that in the first experiment pyridine was still adsorbed on Bronsted acid sites, while these sites were accessible in the second. Since hydrocarbons were only found after the latter pretreatment, the experiment shows the necessity of Bronsted acid sites for that reaction and furthermore that pyridine is capable to adsorb on all acidic sites in the channel structure.

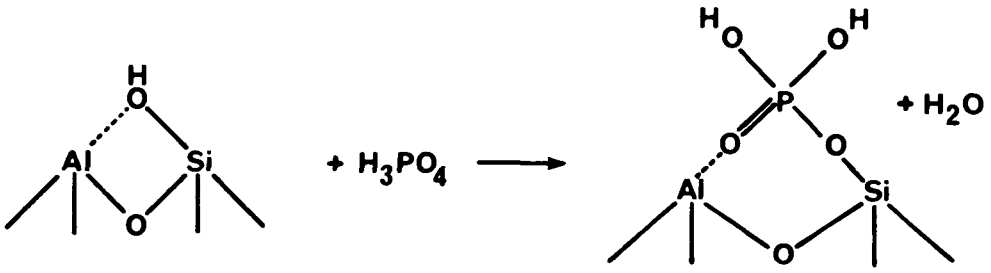

Fig.8. Model of the interaction of H_3PO_4 with Bronsted acid sites

Therefore the selectivities and reactivities found with H_3PO_4 treated ZSM5 zeolites suggest that the strength of all acid sites was diminished and that the weaker Bronsted acid sites found with ZSM5P5 and ZSM5P8 are hardly able to form hydrocarbons from methanol. The decrease in acid strength had (like partial poisoning with pyridine) virtually no influence upon the formation of dimethylether (DME). It indicates that only weak acid sites are needed for DME

formation, but strong for hydrocarbon formation from methanol.

It was reported (17-19) that the modification with H_3PO_4 leads to the modification of the outer and inner surface of the ZSM5 zeolite and that narrowing of the pore mouth and the pores will take place and will cause diffusional constraints. However, the results of cracking of n-hexane show a sharp increase in apparent activation energy with increasing H_3PO_4 loading, which is interpreted as decrease in acid strength and is incompatible with diffusional constraints for n-hexane. In addition, the relative small decrease in BET surface area suggests only small changes of the accessible pore volume of the catalyst. Therefore we are confident that H_3PO_4 entered the catalyst pores.

Since strong Bronsted acid sites could be replaced by rather weak Bronsted acid sites, the place of anchoring the phosphate ions in the zeolite framework should be given by Al^{3+} cations. In another paper, we suggested (in accordance with (20)) that the channel intersections are the most probable locations for these Al^{3+} cations (14).

Speculating, how the phosphate might be anchored (see figure 8) we recognize that the bridging OH group of the zeolite is replaced by two "terminal" hydroxyl groups. Mortier et al.(5) showed that the former type has significantly higher acid strength. Therefore the model proposed, accounts for the decrease in acid strength caused by H_3PO_4 loading.

The effects of H_3PO_4 upon ZSM5 zeolites show again that general relationships, such as Sanderson's electronegativities, have to be used with great care to predict properties of materials. These relationships are very useful to predict the relative strength of a particular group, if neither the type of bonding (as demonstrated here) nor, for the same type of bonding, (shown by Derouane et al. (10)) the bonding geometry has been altered. Both limitations must be handled strictly and are seldom fullfilled, when changing from one class of chemical compounds to another.

ACKNOWLEDGEMENTS

The authors thank J. Lebok, H. Schnait, Ch. Weigel, B. Zeiler and A. Jentys for assistance during measurements as well as the "Fonds zur Förderung der wissenschaftlichen Forschung" for providing the i.r. spectrometer.

REFERENCES

1. Sanderson, R.T.: Chemical Bond and Bond Energy, Academic Press, New York, 1971.
2. Mikheikin, I.D., Abronin, I.A., Zhidomirov, G.M., Kazanskii, V.B., J. Mol. Catal. 3, 435 (1978).
3. Jacobs, P.A., Mortier, W.J., Zeolites 2, 226 (1982).

4. Jacobs, P.A., Martens, J.A., Weitkamp, J., Beyer, H.K., Faraday Discuss. 72, 353 (1981).
5. Mortier, W.J., Sauer, J., Lercher, J.A., Noller, H., J. Phys. Chem. 88, 905 (1984).
6. Lercher, J.A., Noller, H., J. Catal. 77, 152 (1982).
7. Hair, M.L., Hertl, W., J. Phys. Chem. 74, 91 (1970).
8. Chandawar, K.H., Kulkarni, S.B., Ratnasamy, P., Applied Catal. 4, 287 (1982).
9. Young, L.B., Butter, S.A., Kaeding, W.W., J. Catal. 76, 418 (1982).
10. Derouane, E.G., Baltusis, L., Dessau, R.M., Schmitt, K.D. in "Catalysis by Acids and Bases", Elsevier Pub. Co., Amsterdam, 1985.
11. Wilson, S.T., Lok, B.M., Flanigen, E.M., U.S. Patent 4,385,994 (1983) and U.S. Patent 4,310,440 (1982).
12. Latzel, J., Kaes, G., React. Kin. Catal. Lett. 9, 183 (1978).
13. Topsoe, N.Y., Pedersen, K., Derouane, E.G., J. Catal. 70, 41 (1981).
14. Lercher, J.A., Rumplmayr, G., Z. Phys. Chem. NF, submitted.
15. Lercher, J.A., Vinek, H., Noller, H., J. Chem. Soc., Faraday Trans. I 80, 1239 (1984).
Lercher, J.A., Ritter, G., Vinek, H., J. Coll. Int. Sci., in press.
16. Ward, J.W., J. Catal. 10, 34 (1968).
17. Gilson, J.P., Derouane E.G., J. Catal. 88, 538 (1984).
18. Kaeding, W.W., Butter, S.A., J. Catal. 61, 155 (1980).
19. Kaeding, W.W., Chu, C., Young, L.B., Weinstein, B., Butter, S.A., J. Catal. 67, 159 (1981).
20. Babu, G.B., Hedge, S.G., Kulkarni, S.B., Ratnasamy, P., J. Catal. 81, 471 (1983).